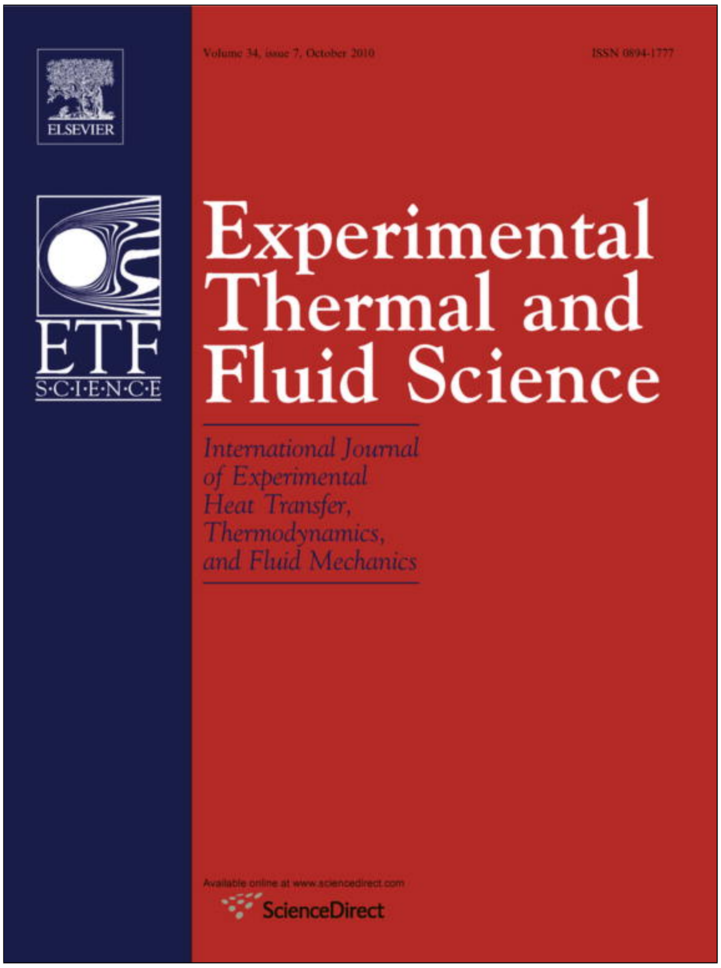
Volume 34, issue 7, October 2010
ISSN 0894-1777
ELSEVIER
ETF
S·C·I·E·N·C·E
Experimental Thermal and Fluid Science
International Journal of Experimental Heat Transfer, Thermodynamics, and Fluid Mechanics
Available online at www.sciencedirect.com
ScienceDirect

Experimental Thermal and Fluid Science 34 (2010) 813–826

Contents lists available at ScienceDirect

Experimental Thermal and Fluid Science

journal homepage: www.elsevier.com/locate/etfs

# The effects of surface tension on flooding in counter-current two-phase flow in an inclined tube

Deendarlianto [a,d,*], Akiharu Ousaka [b], Indarto [a], Akira Kariyasaki [c], Dirk Lucas [d], Karen Vierow [e], Christophe Vallee [d], Kevin Hogan [e]

[a] Department of Mechanical & Industrial Engineering, Faculty of Engineering, Gadjah Mada University, Jalan Grafika No.2 Yogyakarta 55281, Indonesia
[b] Department of Mechanical Engineering, The University of Tokushima, 2-1 Minami Josanjima, Tokushima 770-8506, Japan
[c] Department of Chemical Engineering, Fukuoka University, 8-19-1, Jyonan-ku, Fukuoka 814-0180, Japan
[d] Forschungszentrum Dresden-Rossendorf e.V., Institute of Safety Research, P.O. Box 510 119, D-01314 Dresden, Germany
[e] Department of Nuclear Engineering Texas A&M University, 129 Zachry Engineering Center, 3133 TAMU College Station, TX 77843-3133, USA

ARTICLE INFO

*Article history:*
Received 5 August 2009
Received in revised form 26 January 2010
Accepted 27 January 2010

*Keywords:*
Counter-current two-phase flow
Flooding
Inclined tube
Surface tension
Flooding mechanisms

ABSTRACT

The purpose of the present study is to investigate the effects of surface tension on flooding phenomena in counter-current two-phase flow in an inclined tube. Previous studies by other researchers have shown that surface tension has a stabilizing effect on the falling liquid film under certain conditions and a destabilizing or unclear trend under other conditions. Experimental results are reported herein for air–water systems in which a surfactant has been added to vary the liquid surface tension without altering other liquid properties. The flooding section is a tube of 16 mm in inner diameter and 1.1 m length, inclined at 30–60° from horizontal. The flooding mechanisms were observed by using two high-speed video cameras and by measuring the time variation of liquid hold-up along the test tube. The results show that effects of surface tension are significant. The gas velocity needed to induce flooding is lower for a lower surface tension. There was no upward motion of the air–water interfacial waves upon flooding occurrence, even for lower a surface tension. Observations on the liquid film behavior after flooding occurred suggest that the entrainment of liquid droplets plays an important role in the upward transport of liquid. Finally, an empirical correlation for flooding velocities is proposed that includes functional dependencies on surface tension and tube inclination.



## 1. Introduction

The current work focuses on the dependence of flooding on surface tension for counter-current liquid–gas flow in tubes of various inclinations. Flooding can be defined as the onset of flow reversal of the liquid component which results in an upward co-current flow. While studies by other researchers have indicated significant surface tension effects on the conditions for flooding occurrence, the results have not been consistent. The current work aims to extend the understanding of the physics of the relationship between surface tension and flooding phenomena by clarifying the flooding mechanisms under various values of surface tension for a range of tube inclinations. Such understanding is important because the surface tension varies in applications from that of air–water at room temperature. Industrial applications employ various fluids that have different thermophysical properties. Steam and water in nuclear reactors at higher temperature and pressure will also have a greatly different surface tension. A mechanistic understanding of the role of surface tension will allow for more accurate analysis techniques to promote extended operation and improved safety.

Counter-current two-phase flow in vertical tubes has many applications in a diverse range of process industries. The phenomenon of flooding is of considerable technological importance, as flooding can be a limiting factor in the operation of equipment. For example, in a pressurized water reactor (PWR), the counter-current flow of steam (upward) and cold water (downward) may take place in vertical channels when the emergency core cooling (ECC) water is injected into the reactor vessel. This leads to complex processes including the condensation of steam due to the introduction of cold water into the reactor core. Most importantly, upward steam flow may prevent sufficient cooling of reactor components by the ECC water.

Flooding in inclined channels can also potentially occur in a variety of situations, such as the pressurizer surge line of a PWR. The pressurizer surge line is typically comprised of several sections with various inclination angles. Under certain accident conditions,

* Corresponding author. Address: Forschungszentrum Dresden-Rossendorf e.V., Institute of Safety Research, P.O. Box 510 119, D-01314 Dresden, Germany. Tel.: +49 351 260 2425.
*E-mail addresses:* d.deen@fzd.de, deendarlianto@ugm.ac.id ( Deendarlianto).

0894-1777/$ - see front matter © 2010 Elsevier Inc. All rights reserved.
doi:10.1016/j.expthermflusci.2010.01.010

**Nomenclature**

| | |
|---|---|
| $C$ | constant in Eqs. (6)–(8) (–) |
| $D$ | tube inner diameter (m) |
| $g$ | gravitational acceleration (m/s$^2$) |
| $J_G$ | superficial gas velocity (m/s) |
| $J_{G,f}$ | superficial gas velocity at flooding (m/s) |
| $J_{G,do}$ | superficial gas velocity at complete dry out (m/s) |
| $J_L$ | inlet superficial liquid velocity (m/s) |
| $J_{L,D}$ | discharged superficial liquid velocity (m/s) |
| $J_K^*$ | Wallis dimensionless number of superficial velocity (–) |
| $\mathrm{Ku}_G$ | Kutateledze dimensionless number of the gas phase (–) |
| $L$ | tube length (m) |
| $m$ | constant in Eq. (6) (–) |
| $t$ | time (s) |
| $V'_d$ | dimensionless discharged liquid flow rate (–) |
| $V'_G$ | dimensionless gas flow rate (–) |

*Greek Letter*

| | |
|---|---|
| $\theta$ | inclination angle from horizontal (deg) |
| $\eta$ | liquid hold-up (–) |
| $\rho_k$ | liquid and gas density (kg/m$^3$) |
| $\sigma$ | surface tension (N/m) |
| $\mu$ | static viscosity (Pa s) |

counter-current flow takes place in the surge line with liquid flowing down from the pressurizer vessel and steam flowing up from the hot leg of the reactor pressure vessel. The steam venting rate as well as the liquid draining rate may affect the ECC actuation [20].

Chung et al. [3] reported that the surface tension had a stabilizing effect on flooding, i.e. the flooding gas velocity was lower for a lower surface tension. English et al. [7] found the same trend. However, Kamei et al. [10] found the opposite trend. On the other hand, Suzuki and Ueda [19] reported that the effect of surface tension was complicated and the flooding gas velocity took its maximum value at a surface tension close to $5.0 \times 10^{-2}$ N/m.

While the above studies were performed in vertical tubes, little work has been reported on the effects of surface tension in inclined tubes. Barnea et al. [1] studied air–water counter-current two-phase flow in an inclined tube for a wide range of inclinations (1–90° from horizontal). They reported that the gas velocities upon flooding occurrence increase and then decrease as the tube inclination is changed from horizontal to vertical. Zapke and Kroger [23] investigated the effect of gas and liquid properties upon flooding in inclined tubes, but they only examined a tube inclination of 60°. Next Mouza et al. [15] examined the incipient flooding in inclined tubes of small diameter. In the conclusion of their study, it is suggested that additional data is needed in order to explain the effects of liquids and gases properties on flooding and to assess the significance of dimensionless numbers employed for general correlations. A more detailed survey of the literature for flooding in inclined tubes was performed and a simplified analytical model to predict the optimum channel inclination angle for gas venting has been proposed by Liao and Vierow [12].

Recently, a subset of the authors [6] observed the liquid film behavior upon flooding of an adiabatic counter-current two-phase flow in an inclined tube by using the combination of time variation measurements of liquid hold-up taken along the tube and visual observation. The liquid hold-up is the fraction of the tube cross sectional area occupied by liquid. This work provides the basis for studies of the effects of surface tension in inclined tubes. They reported that there are two prevalent locations of flooding in an inclined tube which are associated with distinct conditions: "lower flooding" and "upper flooding", respectively. The terms lower flooding and upper flooding indicate whether flooding is initiated at the lower or the upper locus of the test section.

Lower flooding occurred at lower liquid flow rate and high tube inclination angle, and the breakdown of the waves at the air–liquid interface occurred in the lower part of the tube ($x/L$ ranged from 0.0 to 0.5). Here, $L$ is the total tube length and $x$ is the distance from liquid outlet. The breakdown of waves is considered as the point of flooding because all the liquid supplied cannot flow down smoothly. It is initiated by the increase of the wave height, in which the wave formation is begun from the upper part of the test tube ($x/L \cong$ unity). The wave height increases with the downward movement. It is disrupted by the air flow when the wave height reaches a certain height in counter-current flow. Liquid droplets arise at nearly the same time of the breakdown of the wave and there is no upward motion in the liquid film.

On the other hand, upper flooding occurred at higher liquid flow rate and low tube inclination. It is initiated by the formation of low void fraction region in the upper part of the test tube ($x/L \cong$ unity), in which the maximum of liquid hold-up is 1.0. For small tube diameters, the liquid slug can completely bridge the cross sectional area of the test tube. It moves downward for a short distance and is broken up by air flow in the upper part of the test tube ($x/L$ from 0.5 to 1.0). Furthermore, it was noticed that there was no reverse motion of the liquid film at the point of flooding during the occurrence of either lower flooding or upper flooding.

The objective of the current work is to carry out a series of flooding measurements for different surface tension values, making detailed observations in each case, to clarify the governing phenomena for flooding and the post-flooding conditions of partial liquid delivery and zero penetration. In this paper, the experimental results of instantaneous liquid hold-up at the point of flooding and afterwards, under a single liquid flow rate, will be presented first for a range of surface tension values. This data will reveal information on the wave growth and the propagation direction of the liquid film. The philosophy of upper flooding and lower flooding, as proposed in the previous papers, will be extended. Next, the effect of surface tension on the gas velocity at flooding and possible explanations will be presented. The effect of surface tension on flow patterns occurring after flooding, namely partial liquid delivery and zero penetration, are also experimentally examined. Finally, an empirical correlation for the onset of flooding gas velocity that incorporates the effect of liquid surface tension is proposed.

## 2. Experimental apparatus and procedures

The details of the experimental apparatus and procedure used in the present study were described in the previous papers [5,6,16] and only the main features are presented here. The test section consisted of a test tube having total length of 1.1 m as shown in Fig. 1. Air was fed from a compressor to the lower end of the inclined tube and flowed upward through the test section to a separator. Liquid entered from a porous section and flowed downward in the tube. The inlet liquid flow rate and the discharged liquid flow rate were both measured. To ensure accuracy, the liquid flow rate was confirmed by collecting the liquid discharged from the lower test tube outlet over a fixed period of time, and the measurements were time-averaged and shown to have good repeatability.

The test tube was made of transparent acrylic resin with an inner diameter of 16 mm. The liquid inlet consisted of a porous sec-

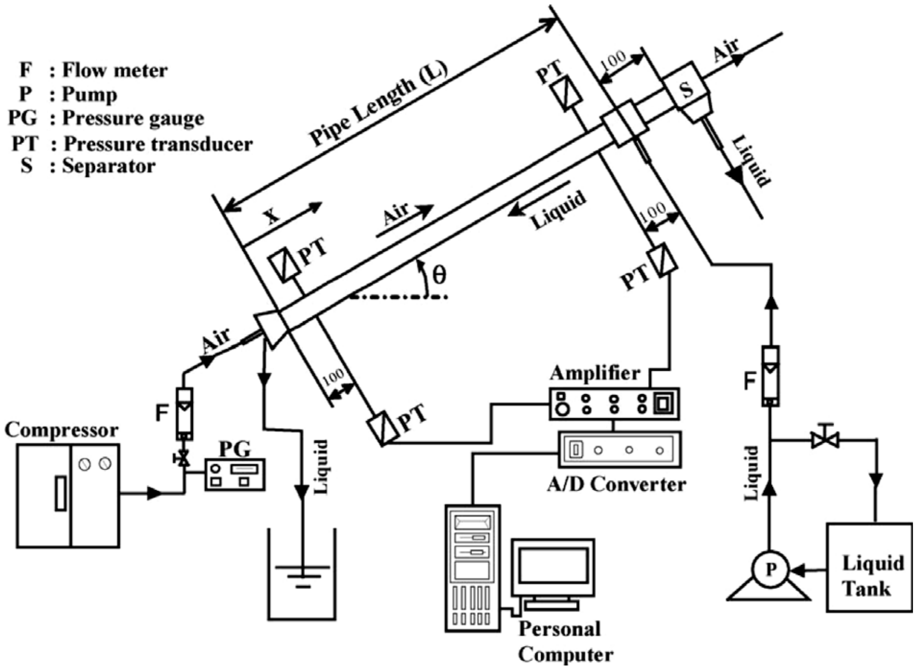


**Fig. 1.** Schematic diagram of experimental apparatus.

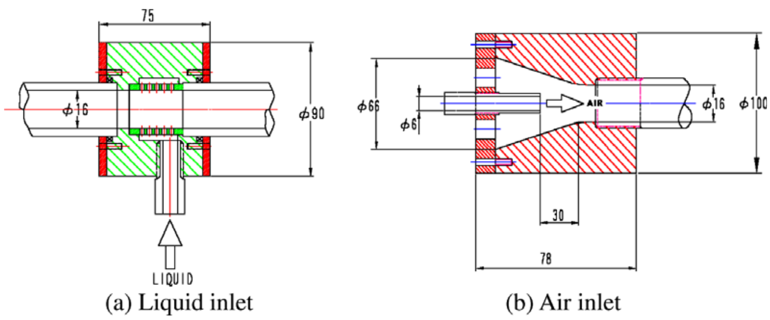


**Fig. 2.** Liquid and air inlets [5].

tion of tube to insure that the liquid film flow was uniform at the point of entry. The air entrance was made of acrylic resin, providing a conical inlet passage to avoid turbulence effects in this section. The schematic drawings of the liquid inlet and the air entrance are shown respectively in Fig. 2a and b.

The experiments were performed using air and three test liquids, i.e., water and aqueous oleic acid natrium solution of two differing concentrations, thus providing test liquids with a variation of surface tension $\sigma_L$. Surface tension was measured using an automatic surface tension measurement system. This system uses a photoelectric sensor to detect a falling drop under the capillary tip. The liquid surface tension is calculated from the volume of the falling drop. The details of the experimental apparatus, principle and the measurement system can be found in [14]. The liquid temperatures were approximately 20 °C and fluid properties are given in Table 1.

In the present study, we used oleic acid natrium to decrease the surface tension because it is a powerful surfactant which, when used in low concentrations (0.1 wt.%), decreases the surface tension to 0.031 N/m without affecting other liquid properties. A typical measurement of the relationship between the surface tension and the weight percentage of oleic acid natrium is shown in Fig. 3. In the present study, the measurements of surface tension were done both at the inlet and the exit of test tube, before and after the experiment. As a result the values of surface tension were almost the same. This indicates the concentration and distribution of surfactant in the test fluids are almost uniform. Consequently, the effect of dynamic surface tension in our experiments can be neglected.

The interfacial behavior of the liquid film was investigated by using two high-speed video cameras. The pictures were taken at different locations along the tube at 240 frames per second and at a shutter speed of 1/10,000 s. During this experimental study, two cameras were used, one at the liquid inlet and another at the liquid outlet.

**Table 1**
Physical properties of liquid used in the experiment (at 20 °C).

| Liquid | $\rho_L$ (kg/m$^3$) | $\sigma_L$ (N/m) | $\mu_L$ (Pa s) |
|---|---|---|---|
| Water (**S72**) | 998.2 | 0.072 | $10.03 \times 10^{-4}$ |
| 0.02 wt.% oleic acid natrium solution (**S72**) | 998.2 | 0.051 | $10.03 \times 10^{-4}$ |
| 0.05 wt.% oleic acid natrium solution (**S34**) | 998.2 | 0.034 | $10.03 \times 10^{-4}$ |

$\rho_L$: density, $\sigma_L$: surface tension and $\mu_L$: static viscosity.

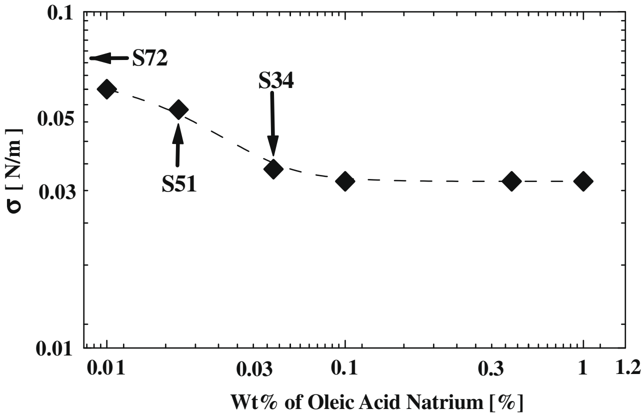


**Fig. 3.** Surface tension vs. weight percentage of oleic acid natrium (at 20 °C).

The instantaneous local liquid hold-up was detected by using the constant electric current method (CECM). The liquid hold-up is the fraction of the tube cross sectional area occupied by liquid. This method works on the basis of the difference in the electric resistance between the gas and the liquid phases. It was originally developed by Fukano [8] to observe the interfacial structure in co-current gas–liquid two-phase upward flow. Furthermore, it was used by the authors to investigate the liquid film behavior during adiabatic air–water counter-current two-phase flow in an inclined tube [6]. In the present experiment, we used six liquid hold-up sensors arranged with an axial spacing of 100 mm. Each sensor consists of a pair of brass electrodes, 1 mm in thickness, 5 mm apart from each other, mounted flush with the inner surface of the test tube. Since the electrodes were mounted flush with the surface of the channel, two-phase flow was not disturbed by the electrodes. The output signals from the sensors were sent respectively through the floating amplifier with high input impedance to a personal computer via an A/D converter. The liquid hold-up data were acquired at 1.0 kHz. Further details of the experimental apparatus, principle and the measurement system can be found in Fukano [8,9].

In the present experiment, the liquid flow rate was kept constant and the airflow rate was increased in small increments. Prior to changing to the next air flow rate, at least a few minutes was allowed to elapse to ensure that the flow pattern was in a steady state. Next, the liquid hold-up, pressure gradient and discharged liquid flow rate were measured. Flooding was defined as the limit of stability of the counter-current flow, indicated by the maximum airflow rate at which the discharged liquid flow rate is equal to the inlet liquid flow rate. Flooding is commonly referred to as the point of transition between counter-current flow and partial delivery.

The experimental conditions were as follows: tube inclinations: 30°, 45° and 60° from horizontal; the range of superficial liquid velocity: $J_L$ = 0.03–0.32 m/s and the superficial gas velocity; $J_G$ = 0.0–14 m/s.

To simplify the explanation in this paper, we have used some abbreviations for the test liquids on the basis of their surface tensions. The abbreviations in this paper are as follows: **S72**: Air–water (static surface tension $\sigma_L$ = 0.072 N/m), **S51**: Air–0.02 wt.% aqueous oleic acid natrium solution ($\sigma_L$ = 0.051 N/m) and **S34**: Air–0.05 wt.% aqueous oleic acid natrium solution ($\sigma_L$ = 0.034 N/m). Furthermore, the abbreviations for the flow characteristics are as follows: **W**: wave, **LW**: large wave, **BW**: breakdown of the wave and **RW**: ring-type of the wave. Here, **LW** corresponds to the blockage of the wave in the test tube, whereas the maximum liquid hold-up of the wave (**W**) is equal to 1.0.

## 3. Results and discussion

### *3.1. Flow behavior in flooding condition*

#### *3.1.1. Low liquid flow rate*

Fig. 4 shows the comparison of the time variation of liquid hold-up for each test liquid at low liquid flow rate, $J_L$ = 0.03 m/s for example. The tube inclination was 30°. In the figure, (a), (b) and (c) correspond to the cases of **S72**, **S51** and **S34** respectively. In the figure, $J_G$ was taken as the superficial gas velocity at the initiation of flooding of each case. In these tests, the fluids were in a stratified flow pattern. From Fig. 4a, it is noted that:

1. The time signature of **W** at $x/L$ = 0.75 and $t \approx 0.03$ s indicates that a wave is formed near the top of the test tube ($x/L \cong$ unity). It then propagates downwards and it is clearly seen from the figure that waves shift to the lower right. Next the liquid hold-up of this wave increases from $x/L$ = 0.75–0.25, indicating that the wave height increases with downward movement. This is behavior that may precede flooding.
2. Next, the breakdown of the wave (**BW**) is observed to occur at $x/L$ = 0.35 and $t \approx 1.64$ s. In this period, the corresponding wave recorded by the sensor at $x/L$ = 0.35 and $t \approx 1.64$ s, the height of which is noticeably higher at $x/L$ = 0.45, seems to be disappearing by the time it reaches the sensor at $x/L$ = 0.35 and $t \approx 1.64$ s. Consequently, the local liquid hold-up at this wave is smaller than the corresponding wave recorded by the previous sensor ($x/L$ = 0.45 and $t \approx 1.61$ s). The occurrence of **BW** under this flow condition is considered to be flooding because all the liquid supplied cannot flow down smoothly [6].

The process of the wave breakdown under this flow condition included the formation of roll wave and the development of entrained liquid droplets as reported in the previous paper [6] is shown in Fig. 5.

Despite the decrease of surface tension to 0.051 and 0.034 N/m as shown in Fig. 4b and c, the phenomena are similar. The waves are initiated at the top of the test tube and propagate downwards, in which the maximum wave height increases as the waves move downstream. Next, the **BW** occurs in the lower part of test tube ($x/L$ ranges from 0.25 to 0.45). From Fig. 4a–c, it is revealed that associated waves continue to travel downward **BW**, signifying that there is no upward motion of the wave even for smaller surface tension. In addition, there is no blockage process in the tube, as the maximum liquid hold-up is smaller than 1.0.

According to the previous paper [6] with higher surface tension, lower flooding occurs under this flow condition. In the current experiments, **BW** occurs in the lower half of the tube. From the above results, it is concluded that the surface tension does not change the flooding location at low liquid flow rate in an inclined tube.

As the airflow is increased further, the discharged liquid flow rate becomes smaller than the inlet liquid flow rate, and the chaotic regions, i.e. the generation and the breakdown of the waves extend further along the length of the tube. Evidence is shown clearly in Fig. 6, in which (a) and (b) correspond to the cases of **S72** and **S51** respectively. The discharged liquid flow rate under the flow conditions in Fig. 6a and b are 89% and 91% of the inlet liquid flow rate. Close inspection of these figures reveal that there is no flow reversal of waves under these flow conditions, because the wave's signs of the liquid hold-up signal always shift to the lower right. This poses the question, how does the discharge liquid flow rate become smaller? From visual observation, it can be seen that the upward transport of liquid corresponds to the carry-over of liquid in the form of entrained droplets. After flooding, the droplet

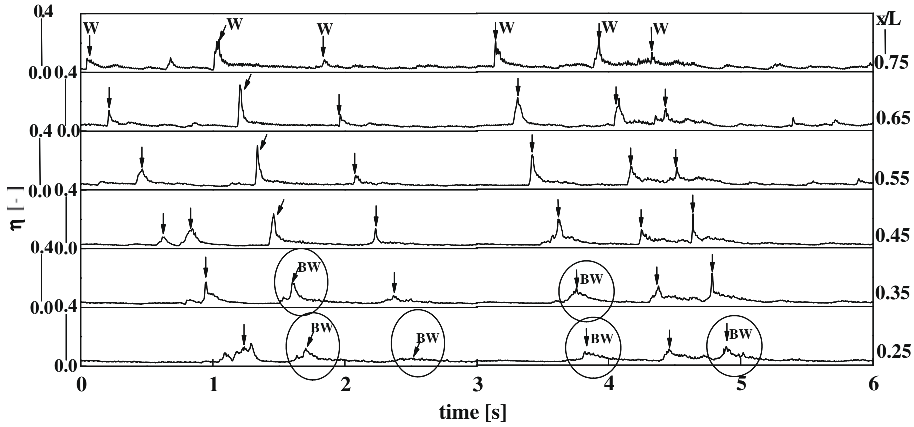


(a) **S72** ($J_L$=0.03 m/s, $J_G$=8.29 m/s and θ=30°).

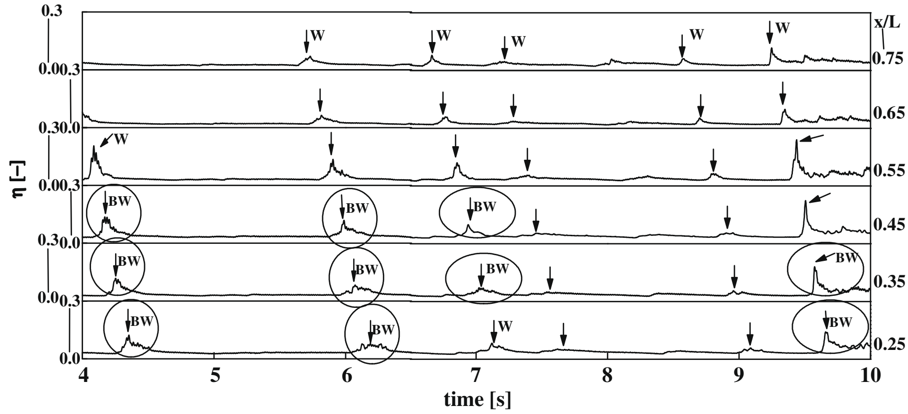


(b) **S51** ($J_L$=0.03 m/s, $J_G$=6.64 m/s and θ=30°).

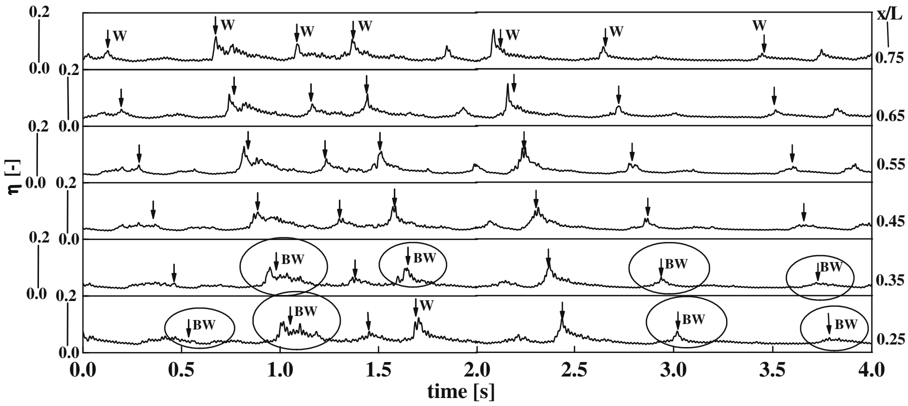


(c) **S34** ($J_L$=0.03 m/s, $J_G$=5.21 m/s and θ=30°).

**Fig. 4.** Comparison of time variation of liquid hold-up at flooding at low liquid flow rate for each surface tension ($J_L$ = 0.03 m/s, $\theta$ = 30° and $L$ = 1.1 m).

flux increases as the gas flow rate increases, making the discharged liquid flow rate decrease gradually. The examples of the interfacial behavior of **S72** taken at $x/L \cong 0.25$ under these flow conditions are shown in Fig. 7. In the figure, the occurrence of the droplet as a result of the breakdown of the wave can also be seen further. The result obtained agrees well with that of Celata et al. [2] who reported that the entrainment effect can completely prevent the liquid from falling down in inclined tubes. From the above results, it is noticed that the flow behavior after flooding at low liquid flow rate does not also fundamentally change if the surface tension is changed from 0.072 to 0.034 N/m.

*3.1.2. High liquid flow rate*

Fig. 8 shows the flow phenomena at flooding at $J_L$ = 0.25 m/s, in which (a), (b) and (c) correspond to the cases of **S72**, **S51** and **S34** respectively. This represents the flow phenomena at high liquid flow rate. From Fig. 8a, the important characteristics' can be described as follows:

1. A large wave, marked as **LW** (the liquid hold-up is about 1.0), is detected occasionally at $x/L$ = 0.75 and $t \approx 1.9$ s. This large wave blocks the whole cross section of the test tube. It is broken up by the airflow at $x/L$ = 0.65 as indicated, **BW** and

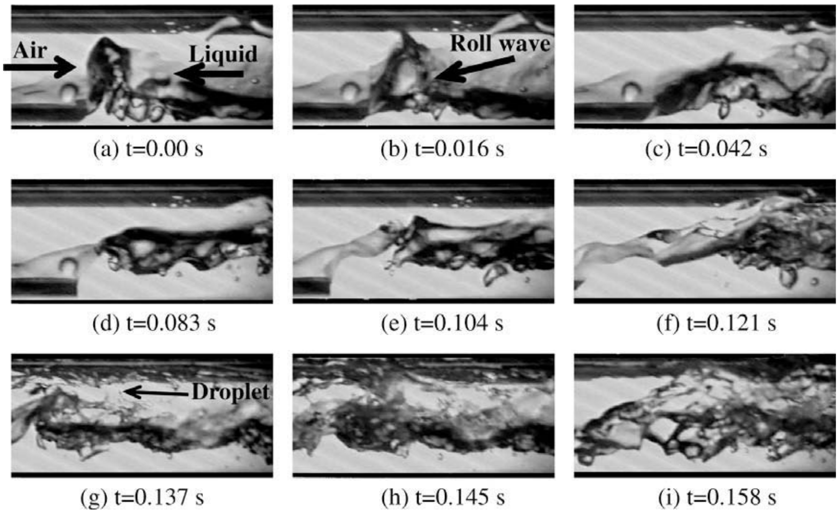


**Fig. 5.** Breakdown of the wave at flooding obtained at $x/L \cong 0.25$ (**S72**, $J_L = 0.03$ m/s, $J_G = 8.29$ m/s, $\theta = 30°$ and $L = 1.1$ m).

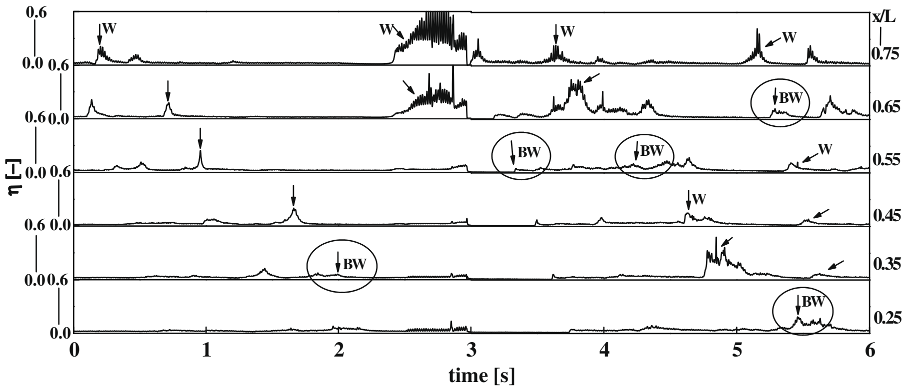


(a) **S72** ($J_L$=0.03 m/s, $J_G$=9.21 m/s and θ=30°).

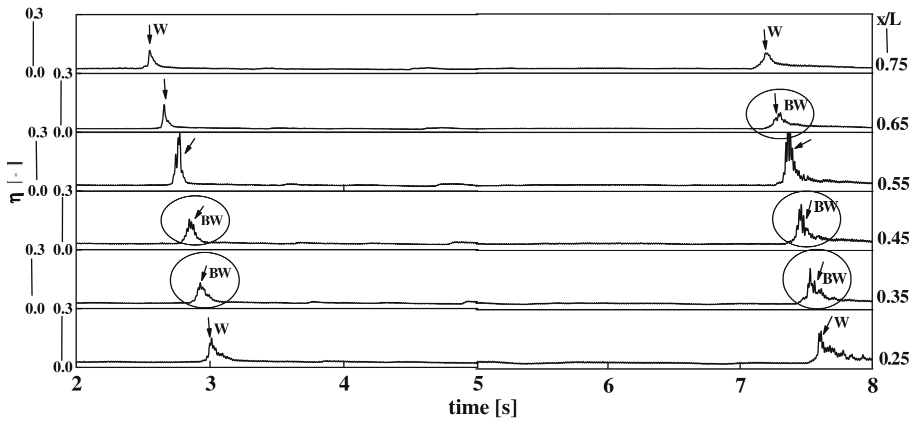


(b) **S51** ($J_L$=0.03 m/s, $J_G$=7.64 m/s, and θ=30°).

**Fig. 6.** Time variation of liquid hold-up after the flooding.

produces smaller waves that move downward along the tube without the reversal motion of the wave. The sequence picture of the wave breakdown under this flow condition obtained near the liquid inlet is shown in Fig. 9. However, in the lower part of the tube the liquid flow flows downwards normally without any broken down of the wave (**BW**) as shown in Fig. 10. The above results indicate that the flooding mechanism under this flow condition is upper flooding, initiated by the sudden formation and the breaking down of a large wave that completely blocks the whole cross section of the test tube in the upper part [6].

With decrease of surface tension to **S51** and **S34**, the flooding mechanism changes drastically as given respectively in Fig. 8b and c. In comparison with Fig. 8a where **S72** is the test liquid, the following is noteworthy:

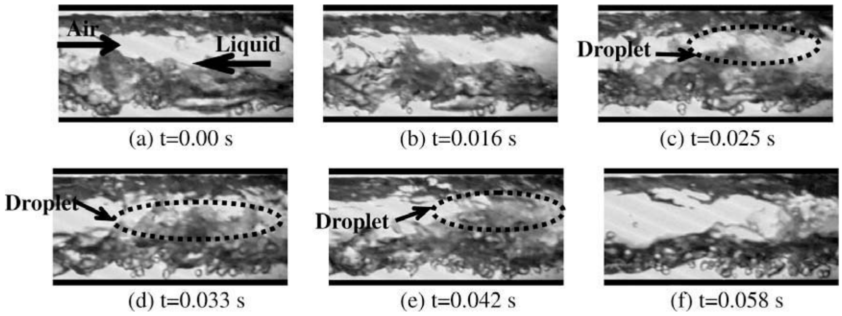


**Fig. 7.** Interfacial behavior of liquid film after the flooding taken at $x/L \cong 0.25$ (**S72**, $J_L = 0.03$ m/s, $J_G = 9.21$ m/s, $\theta = 30°$ and $L = 1.1$ m).

1. Wave formation begins at the top of the test tube. Next, the breakdown of the wave (**BW**) is observed to occur in the lower part of the test section. In the present study, the location of **BW** ranged from $x/L \cong 0.25$ to 0.45. Next, the corresponding wave always shifts to the lower right even after the **BW**, indicating there is no occurrence of upward motion of the wave at the onset of flooding. Evidence is shown clearly in Fig. 8b and c. At the upper part of the test tube the wave flows downwards normally without the blockage process, and is similar to the flow configuration seen before flooding. Evidence is shown in the interfacial behavior of **S72** in Fig. 10.
2. The blockage process caused by a large wave, found in the case of **S72,** did not occur in the cases of **S51** and **S34**. This result indicates that at high liquid flow rate the flooding mechanism changes from upper flooding to lower flooding as the surface tension decreases. The possible reason is due to differences of interfacial behavior of the liquid film near the liquid inlet among the liquids tested. In the case of **S72**, standing waves with short wave length were observed at low gas flow rate. An increase in the gas flow rate causes further wave growth and blockage in the upper part of test tube. On the other hand, the standing waves disappeared when **S51** and **S34** were used. Here the formation of ring-type waves is observed near the liquid inlet. This wave type is shown in Fig. 11, in which it is marked as **RW**. The waves extend 360° around the inner surface of the tube. This ring-type wave is maintained for some distance (10–18 cm) and the liquid film then quickly drains down the wall of the tube, converging at the bottom of the tube to form a stratified wavy layer. The maximum of this wave height increases with downward movement. It will be broken by gas flow at the lower part of the tube if it reaches the certain value of the wave height in counter-current two-phase flow. This result is partly agreement with Mouza et al. [15] who examined the physical properties effect on the incipient of flooding in inclined tubes. They reported that the lower surface tension facilitates lateral liquid spreading and the formation of the waves. Lateral spreading of liquid at flooding appears to take place but the upward moving waves are rather asymmetric with more liquid at the tube bottom. The occurrence of this ring-type of the wave in the cases of lower surface tension is also recorded visually in our experiment, but the upward moving wave at the bottom was not observed. The use of visual observation only in their experiment may lead to the different conclusion. The sketches of interfacial behavior of the liquid film for test liquids are given in Fig. 12.

Fig. 13 shows the comparison of time variation of liquid hold-up after flooding at high liquid flow rate. The flow conditions were $J_L = 0.24$ m/s, $J_G = 6.63$ m/s and $\theta = 30°$. Analysis of this figure is needed in order to determine the upward transport method of liquid film and the effect of surface tension. Close observation of the figures reveals that there is no flow reversal of waves under this flow condition even though the surface tension is decreased, whereas the corresponding wave shifts to lower right. Next, the chaotic region such as the generation and the breakdown of waves encompasses the total length of the test tube. Visual observations reveal that the entrainment of liquid droplets occurs along the tube. From the results, it is concluded that the entrainment of liquid droplets plays an important role in the upward transport of the liquid film, and there is no effect of surface tension.

The flooding locus represented by the wave breakdown locations upon flooding using the visual observations and the analysis of time variation of liquid hold-up are summarized in Fig. 14, in which (a), (b) and (c) correspond to the cases of $\theta = 30°$, 45° and 60° respectively. In most cases, as the liquid flow rate is increased, the flooding locus moves to the upper part of the tube length. The flooding location moves to the lower part of the tube as the surface tension is decreased. In addition, the locus of wave breakdown moves to the lower part of the tube as the tube inclination increases for all test liquids. This result agrees well with that of Deendarlianto et al. [6] who reported the same trend in the longer tube (2.2 m).

### 3.2. Fluid characteristics in flooded condition

The experimental results of discharged liquid flow rate are presented in Figs. 15–17, in which (a), (b) and (c) correspond to the cases of $\theta = 30°$, 45° and 60° respectively. In the figures, the liquid flow rate collected at the lower end of test tube, expressed as the discharged superficial liquid velocity, $J_{L,D}$, is plotted vs. the superficial gas velocity, $J_G$. Flooding is marked by the arrows. The point in which the discharged superficial liquid velocity becomes zero is defined as the zero liquid penetration, marked as **ZP** in the figures. Furthermore, the region between flooding and **ZP** is defined as the partial delivery region.

From the figures it is revealed that the measured discharged liquid flow rate was identical to the inlet liquid flow rate when the flow condition was not flooding or post-flooding (partial liquid delivery or zero penetration). Next the discharged superficial liquid velocities after flooding decrease gradually and the shapes of the curves are independent of the inlet liquid flow rate. Our calculation confirmed that the maximum reduction in the discharged liquid flow rate as the increase of superficial gas velocity $\left(\frac{\Delta J_{L,D}}{\Delta J_G}\right)$ in the partial delivery region was 10.6%. In addition, the trend is similar to all test liquid and tube inclination. This result agrees well with that obtained by Zabaras and Dukler [22] and Lacy and Dukler [11] who showed a gradual decrease in the downward flow rate when the air flow rate was increased beyond the flooding point. On the other hand, this is contradictory to the obtained result by Clift et al. [4] who performed the experimental study on flooding in wetted wall columns. They reported that the down flow rate drops to a value which is sometimes as low as a fifth of down flow imme-

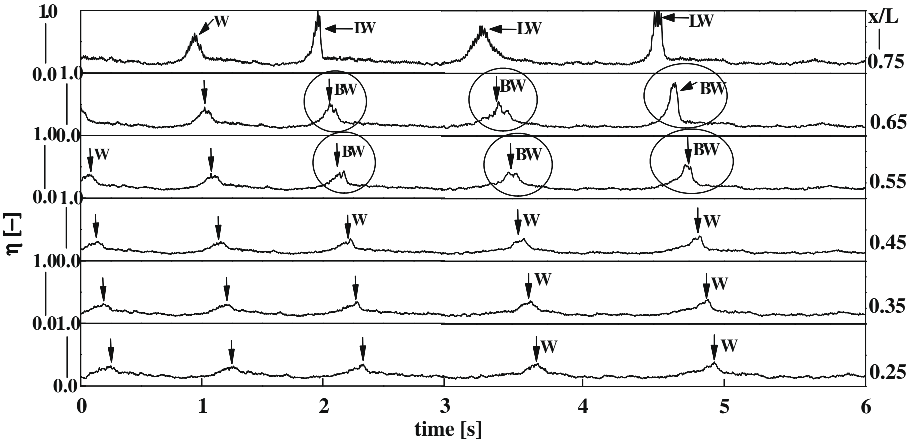


(a) **S72** ($J_L$=0.25 m/s, $J_G$=2.07 m/s and θ=30°).

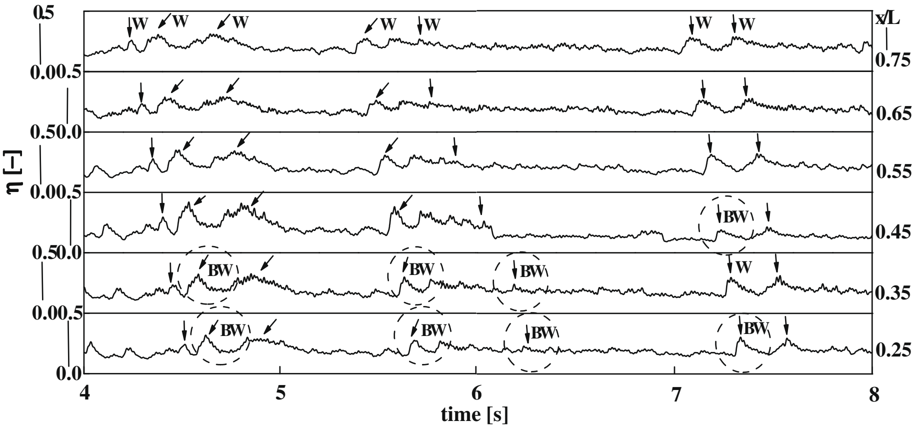


(b) **S51** ($J_L$=0.25 m/s, $J_G$=1.24 m/s and θ=30°).

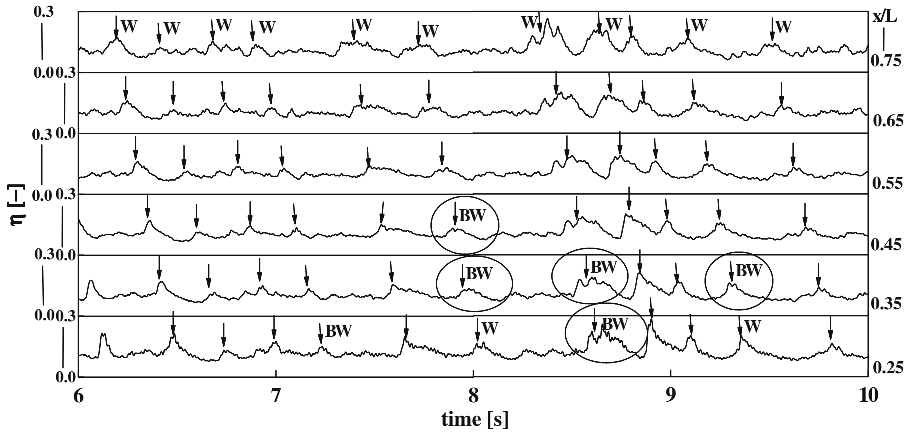


(c) **S34** ($J_L$=0.25 m/s, $J_G$= 0.83 m/s and θ=30°).

**Fig. 8.** Comparison of time variation of liquid hold-up at flooding at high liquid flow rate for each surface tension ($J_L$ = 0.03 m/s and $\theta$ = 30°).

diately before flooding. This may be due to the difference in tube diameter, tube orientation and upward transport method of liquid film. In the present study, we used an inclined tube of 16 mm ID while Clift et al. used a vertical tube of 31.75 mm ID The difference of tube inner diameter affects the upward transport of liquid film [18]. In the present study, it was found that the entrainment of liquid droplets is the primary mechanism for upward flow; while Clift et al. found that the carry up of a liquid slug dominates.

Maharudrayya and Jayanti [13] studied the discharged liquid flow rate behavior in the partial delivery region in vertical pipes. They proposed the dimensionless numbers to correlate them in terms of dimensionless discharged liquid flow rate, $V'_d$ and dimensionless air flow rate, $V'_G$ defined, respectively, as

$$V'_d = \frac{J_{L,D}}{J_L} \tag{1}$$

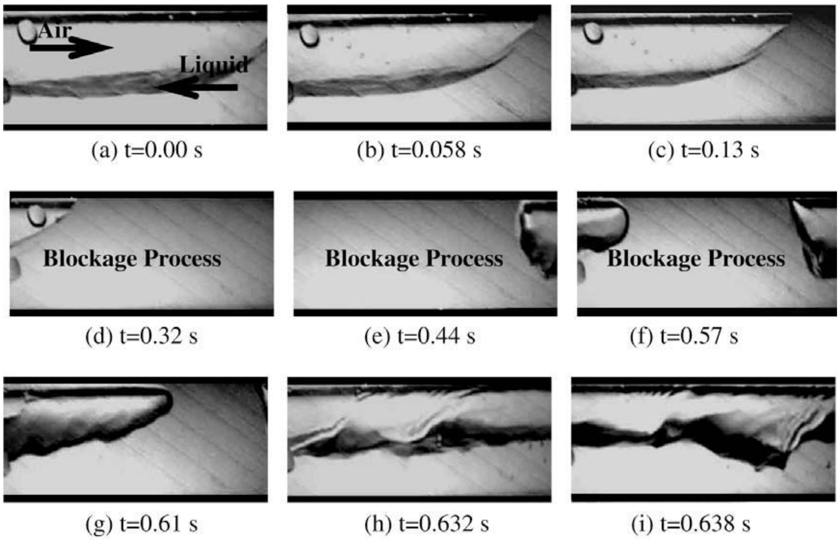


**Fig. 9.** Interfacial behavior at flooding of **S72** at high liquid flow rate obtained at $x/L \cong 0.90$ ($J_L = 0.25$ m/s, $J_G = 2.07$ m/s and $\theta = 30°$).

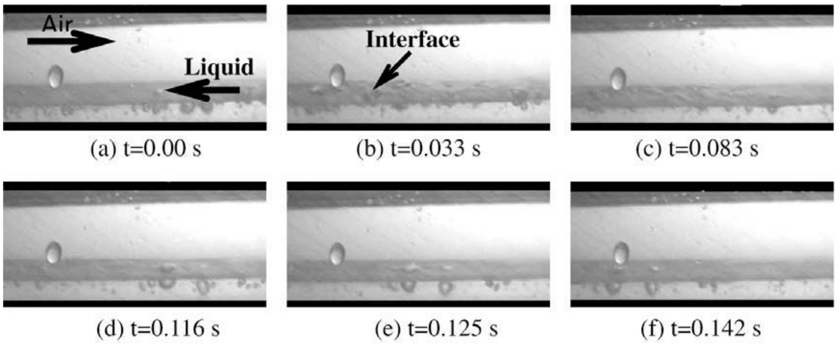


**Fig. 10.** Interfacial behavior at flooding of **S72** at high liquid flow rate obtained at $x/L \cong 0.08$ ($J_L = 0.25$ m/s, $J_G = 2.07$ m/s, $\theta = 30°$ and $L = 1.1$ m).

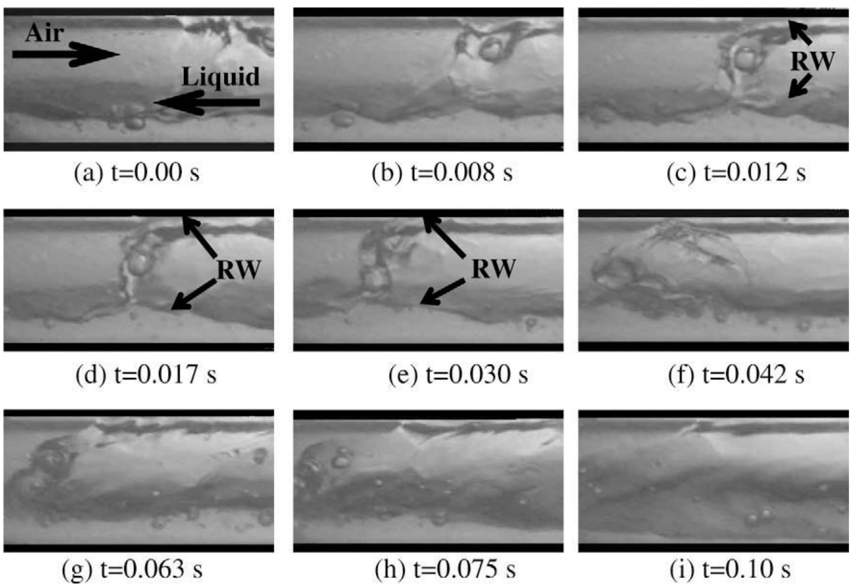


**Fig. 11.** Interfacial behavior of **S51** at flooding obtained near the liquid inlet ($J_L = 0.25$ m/s, $J_G = 1.24$ m/s, $\theta = 30°$ and $L = 1.1$ m).

$$V'_G = \frac{J_G - J_{G,f}}{J_{G,do} - J_{G,f}} \quad (2)$$

where $J_{G,f}$ is the superficial gas velocity at flooding and $J_{G,do}$ is the superficial gas velocity at complete dry out. They recommends that

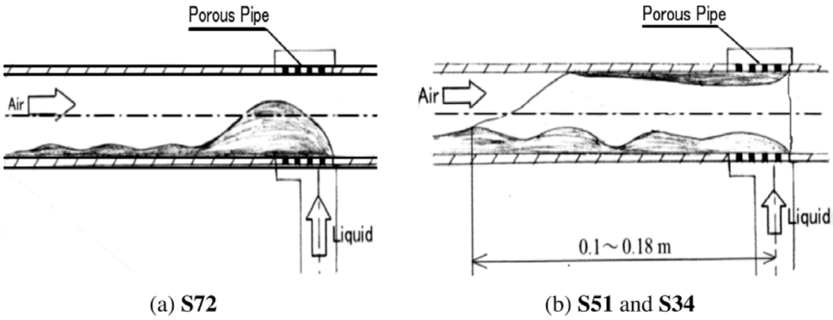


**Fig. 12.** Sketches of interfacial behavior of the test liquids near the liquid inlet ($J_L$ = 0.25 m/s and $\theta$ = 30°).

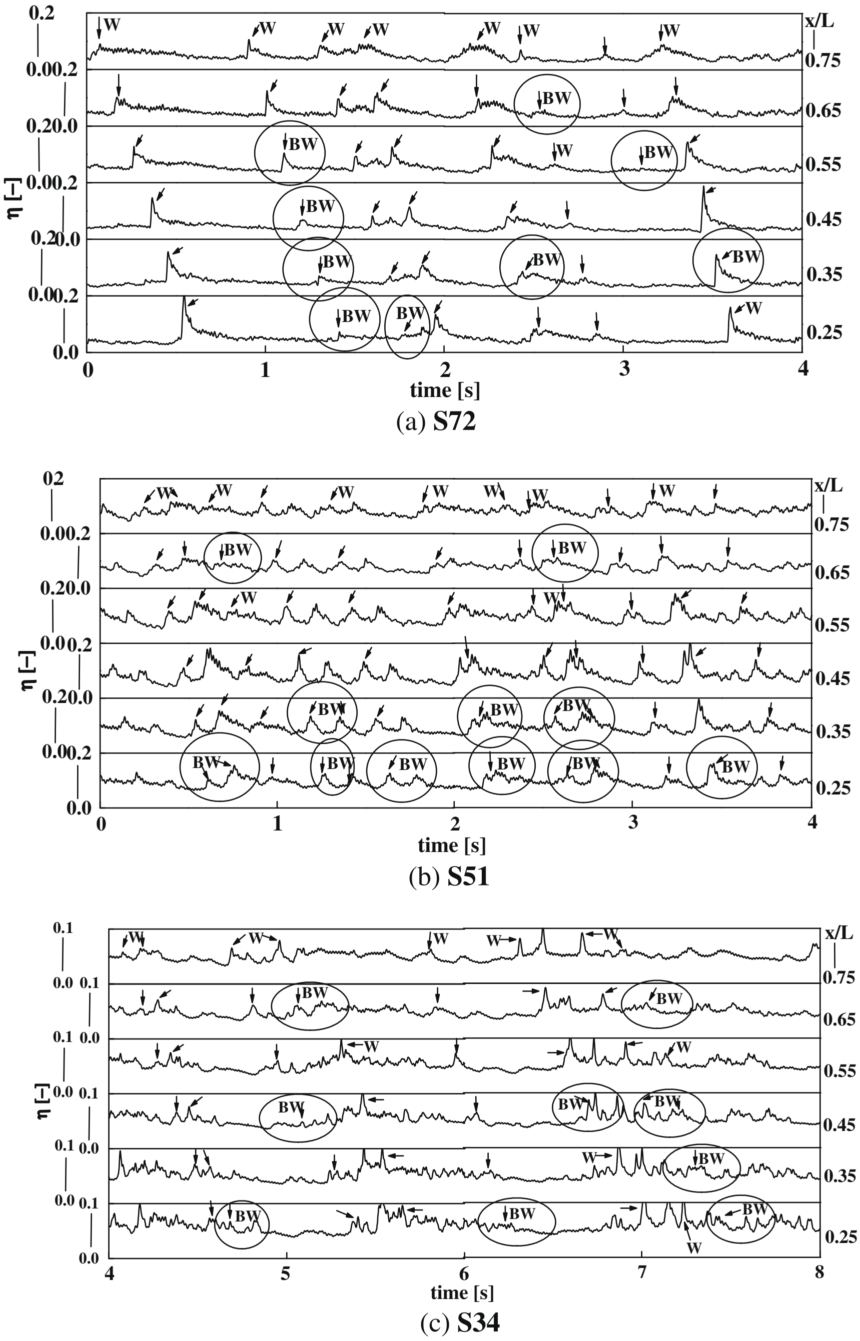


**Fig. 13.** Comparison of time variation of liquid hold-up after the flooding at high liquid flow rate for each surface tension ($J_L$ = 0.25 m/s, $J_G$ = 6.63 m/s and $\theta$ = 30°).

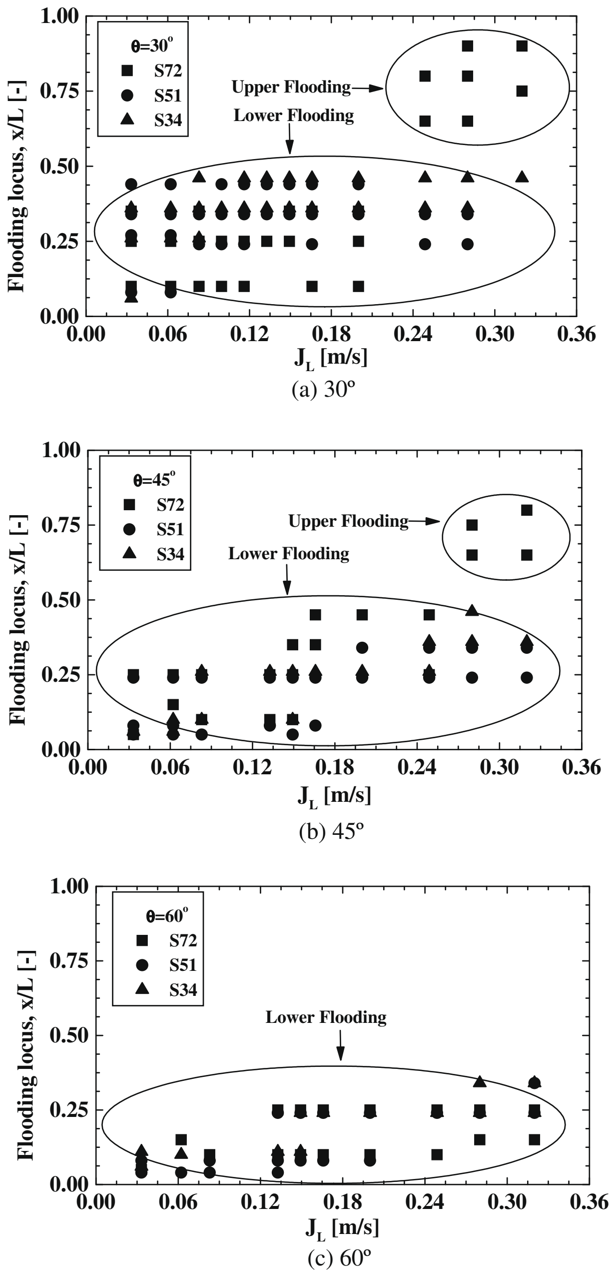


**Fig. 14.** The effect of surface tension on the locus of wave breakdown at flooding.

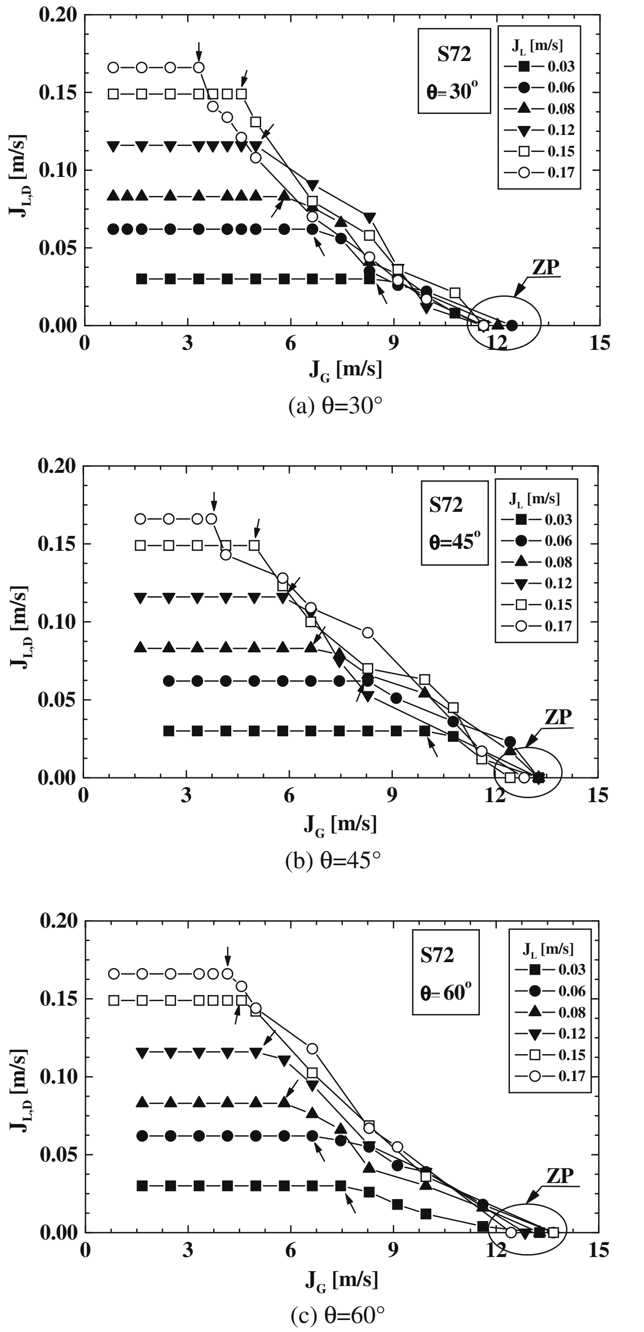


**Fig. 15.** Discharged superficial liquid velocity vs. superficial air velocity of **S72**.

the dry out is taken to be equal to $J_G^* = 1.0$, which is sometimes taken as the criterion for the onset of annular flow. Furthermore they also claimed that the discharged liquid flow rate in the partial delivery region in vertical tube can be correlated as follows:

$$(V'_d)^{0.6} + (V'_G)^{0.6} = 1.0 \tag{3}$$

In Fig. 18, the dimensionless liquid flow rate in the partial delivery region is plotted vs. the corresponding dimensionless air flow rate as proposed by Maharudrayya and Jayanti. From this figure, it is worth noting that the experimental data can be correlated using these dimensionless numbers in which they are independent of tube inclination and surface tension. In comparison with Eq. (4), it is revealed that correlation given by Maharudrayya and Jayanti underestimates the present experimental data. On the other hand, the present experimental data can be correlated as follows:

$$(V'_d)^{0.6} + 0.72(V'_G)^{0.6} = 1.13 \tag{4}$$

Regarding flooding, Wallis [21] proposed the dimensionless number, $J_K^*$, in terms of the gas and liquid superficial velocities to correlate the gas velocity at flooding in vertical tubes. It is defined as follows:

$$J_K^* = J_K\sqrt{\frac{\rho_K}{gD(\rho_L - \rho_G)}} \tag{5}$$

where subscript $K$ indicates gas and liquid phases, $\rho$ the density and $D$ the inner tube diameter. The correlation is expressed as,

$$(J_G^*)^{1/2} + m(J_L^*)^{1/2} = C \tag{6}$$

The constants $m$ and $C$ depend on the inlet and outlet conditions for the liquid phase.

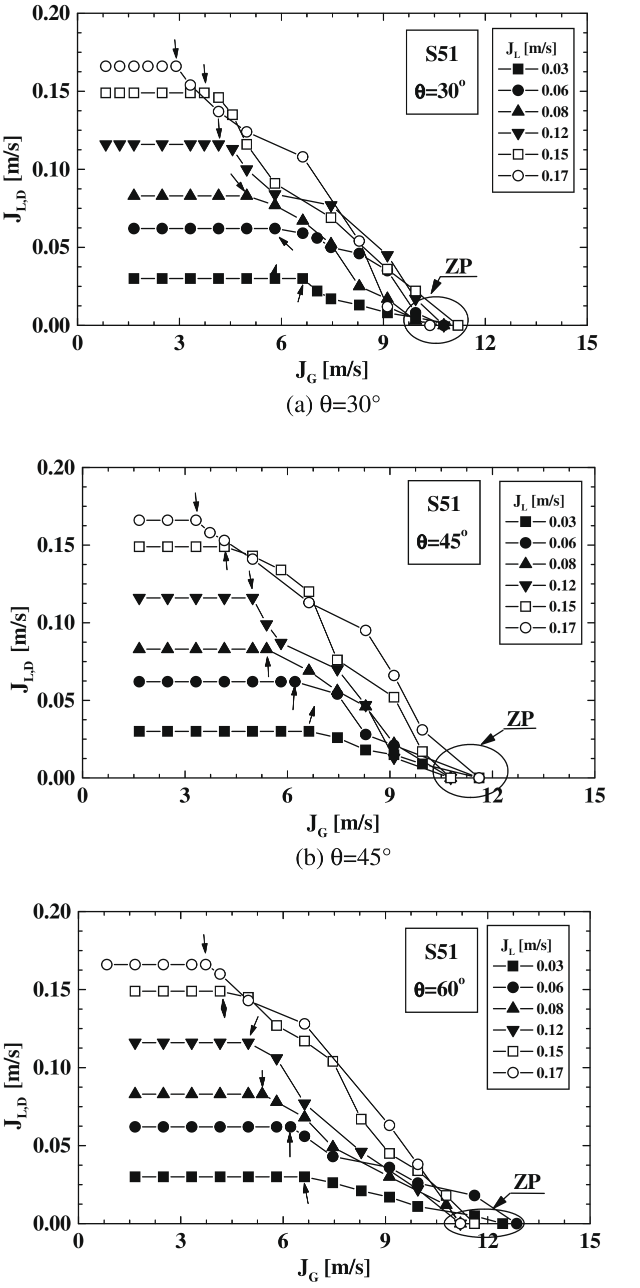


(a) θ=30°

(b) θ=45°

(c) θ=60°

**Fig. 16.** Discharged superficial liquid velocity vs. superficial air velocity of **S51**.

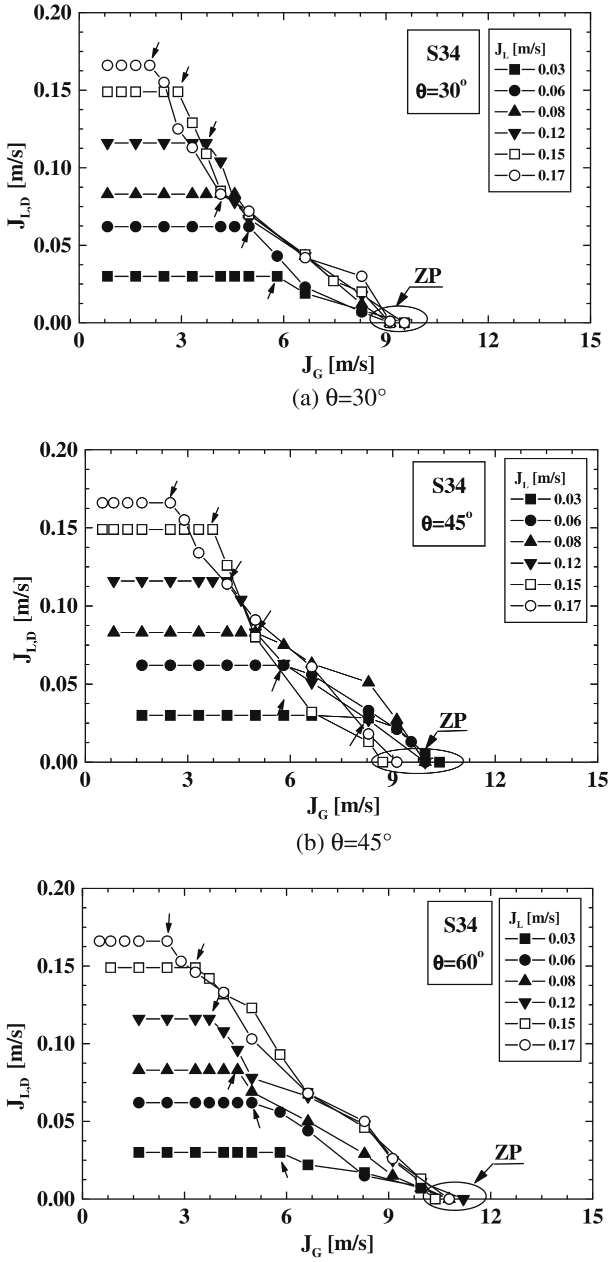


(a) θ=30°

(b) θ=45°

(b) θ=60°

**Fig. 17.** Discharged superficial liquid velocity vs. superficial air velocity of **S34**.

In Fig. 19, the dimensionless superficial gas velocity at flooding is plotted vs. the corresponding superficial liquid velocity as proposed by Wallis. Parameters in this figure are the surface tension and the tube inclination angle. From this figure, it is found that the flooding velocity decreases as the surface tension decreases for all the examined tube inclinations. This trend is same as reported in the literature for tests using vertical tubes [7,3]. In the previous paper, the authors [5] reported that before flooding, the maximum liquid hold-up strongly depends on the surface tension. For given air and liquid flow rates, it increases as the surface tension decreases. Here the maximum liquid hold-up relates to the available gas flow area in counter-current two-phase flow. The higher liquid hold-up means the higher the drag between gas and liquid. Therefore the wave breakdown and flooding will occur at a smaller gas flow rate.

From Fig. 19, slope of the flooding curves are confirmed to be strong functions of the inclination angle. From the above facts, it is easily understood that the surface tension and the tube inclination angle affect the flooding strongly. The flooding data can be correlated by a Wallis-type equation for different surface tension and tube inclination angle

$$(J_G^*)^{1/2} + m(\theta^*)(J_L^*)^{1/2} = C \tag{7}$$

where

$$\left.\begin{aligned} m(\theta^*) &= 1.14(\theta^*)^2 - 1.21\theta^* + 1.01 \\ C &= 0.24\left(\frac{\sigma}{\sigma_W}\right) + 0.82 \\ \theta^* &= \frac{\theta}{90} \end{aligned}\right\} \tag{8}$$

where $\theta$ is the inclination angle from the horizontal axis, $\sigma$ is surface tension of the liquid used and $\sigma_W$ is that of water at room temperature (0.072 N/m) in air. Next, the straight and dotted lines

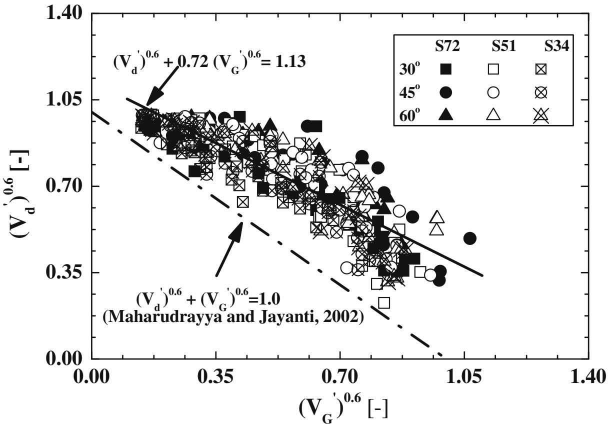


Fig. 18. Comparison of experimental data on discharged liquid flow rate in partial delivery region with Maharudrayya and Jayanti [13] correlation.

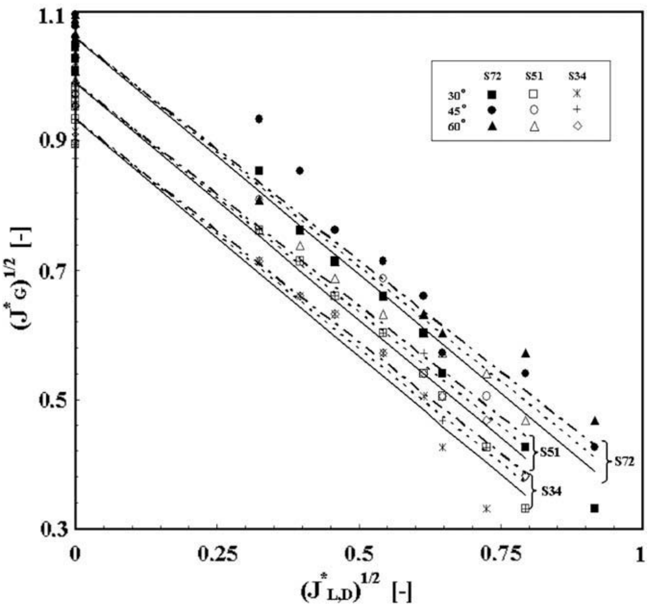


Fig. 19. The onset of flooding.

in the figure are expressed by the above equation. Almost all the data are scattering close together with the lines. The present analysis is a numerical fit to the experimental data. Theoretical modeling, including development of appropriate dimensionless parameters for a new model, may be done as future work.

The zero liquid penetration (**ZP**) was reached when the liquid flow rate at the liquid outlet is zero. This then represents the gas flow rate at which no counter-current flow can exist, i.e. the so called "dry out" point [4]. To the authors' knowledge, the zero liquid penetration in an inclined tube has not been reported in the literature where most of the data have been obtained with vertical tubes. In Fig. 20, the superficial air velocity at zero liquid penetration for specific inlet superficial liquid velocities with different surface tensions and tube inclination is given. The zero liquid penetration is independent of inlet liquid flow rate. This result confirms the conclusions of Clift et al. [4] and Pushkina and Sorokin [17], who performed the experimental study in vertical tubes. On the other hand **ZP** depends strongly on the surface tension and tube inclination. It increases with the tube inclination and decreases as the surface tension decreases. Furthermore, $(J^*_G)^{1/2}$ at zero liquid penetration obtained by Pushkina and Sorokin for a vertical tube takes higher values than those in inclined tubes. From this result it is concluded that the zero liquid penetration takes a maximum value at $\theta = 90°$.

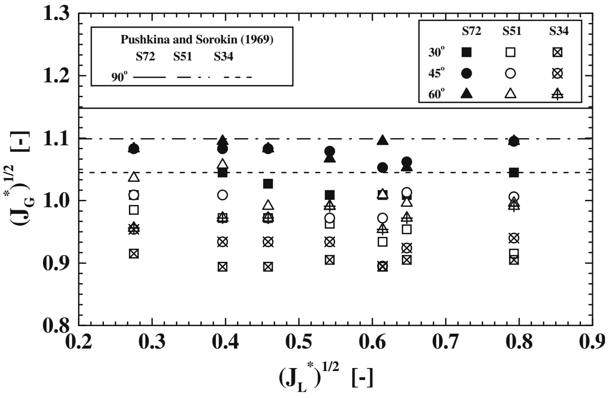


Fig. 20. Zero liquid penetration.

## 4. Conclusions

The effects of the surface tension on flooding phenomena in an inclined tube were investigated experimentally. The tube inner diameter and tube length were 16 mm and 1.1 m, respectively. The experiments were carried out using water and aqueous oleic acid natrium solutions as test liquids. The results are summarized as follows:

1. Surface tension significantly affects the flooding mechanisms in inclined tubes at high liquid flow rate, in that upper flooding changes to lower flooding as the surface tension decreases. Tube blockage by water or a two-phase mixture was seen at high surface tension but not at low surface tension.
2. For low liquid flow rates, the effect of surface tension on flooding in inclined tubes is minimal. The flooding location did not change.
3. At flooding for low surface tension, droplet entrainment plays an important role in the upward transport of liquid.
4. The superficial gas flooding velocity decreases as the surface tension decreases.
5. The Wallis correlation was used as the basis for a simple empirical correlation to predict the flooding gas velocity, accounting for the effects of surface tension and tube inclination angle, as written in Eqs. (7) and (8).
6. Zero liquid penetration is more likely to be observed at greater tube inclination and higher surface tension.


## Acknowledgments

The authors would like to thank Mr. Keisuke Konishi and Mr. Masafumi Konishi, the graduate students of the mechanical engineering of Tokushima University at that time for contributing to the performance of the experiments and technician Jiro Yamashita, for his contribution to the manufacture of the experimental devices.


## References


[1] D. Barnea, N. Ben Yoseph, Y. Taitel, Flooding in inclined pipe: effect of entrance section, The Canadian Journal of Chemical Engineering 64-2 (1986) 177–184.
[2] G.P. Celata, M. Cumo, T. Setaro, Flooding in inclined pipes with obstructions, Experimental Thermal and Fluid Science 5 (1992) 18–25.

[3] K.S. Chung, C.P. Liu, C.L. Tien, The mechanism of flooding in vertical counter-current two-phase flow physico chem, Hydrodynamics 1 (1980) 209–220.

[4] R. Clift, C. Pritchard, R.M. Nedderman, The effect of viscosity on the flooding conditions in wetted wall columns, Chemical Engineering Science 21 (1966) 87–95.

[5] Deendarlianto, A. Ousaka, A. Kariyasaki, T. Fukano, M. Konishi, The effects of surface tension on the flow pattern and counter-current flow limitation (CCFL) in gas-liquid two-phase flow in an inclined pipe, Japanese Journal of Multiphase Flow 18-4 (2004) 337–350.

[6] Deendarlianto, A. Ousaka, A. Kariyasaki, T. Fukano, Investigation of liquid film behavior at the onset of flooding during adiabatic counter-current air–water two-phase flow in an inclined pipe, Nuclear Engineering and Design 235-11 (2005) 2281–2294.

[7] K.G. English, W.T. Jones, R.C. Spillers, V. Orr, Flooding in a vertical updraft partial condenser, Chemical Engineering Progress 59-7 (1963) 51–54.

[8] T. Fukano, Characteristics of Pulsation of Gas-liquid Two-phase Upward Flow, Dr. Thesis, Kyushu University, 1971 (in Japanese).

[9] T. Fukano, Measurement of time varying thickness of liquid film flowing with high speed gas flow by a constant electric current method (CECM), Nuclear Engineering and Design 184 (1998) 363–377.

[10] S. Kamei, J. Onishi, T. Okane, Flooding in a wetted wall tower, Chemical Engineering 18 (1954) 364–368 (in Japanese).

[11] C.E. Lacy, A.E. Dukler, Flooding in vertical tubes – I: experimental studies of the entry region, International Journal of Multiphase Flow 20-2 (1994) 219–233.

[12] Y. Liao, K. Vierow, Optimum channel inclination for gas venting under countercurrent flow limitations, in: Proceedings of the Fourteenth International Conference on Nuclear Engineering – 14 (ICONE-14), Miami, FL, Paper ICONE14-89665, July 17–20, 2006, 7pp.

[13] S. Maharudrayya, S. Jayanti, Investigation of post-flooding conditions in counter-current gas-liquid flow, AIChE Journal 48-2 (2002) 212–220.

[14] H. Matsuki, S. Kaneshina, Y. Yamashita, K. Motomura, Automatic surface tension measurements of aqueous surfactant solutions by the drop volume method, The American Chemical Society 10-11 (1994) 4394–4396.

[15] A.A. Mouza, S.V. Paras, A.J. Karabelas, Incipient flooding in inclined tubes of small diameter, International Journal of Multiphase Flow 29-9 (2003) 1395–1412.

[16] A. Ousaka, Deendarlianto, A. Kariyasaki, T. Fukano, Prediction of flooding gas velocity in gas–liquid counter-current two-phase flow in inclined pipes, Nuclear Engineering and Design 236-12 (2006) 1282–1292.

[17] O.L. Pushkina, Y.L. Sorokin, Breakdown of liquid film motion in vertical tubes, Heat Transfer Soviet Research 1 (1969) 56–64.

[18] M. Vijayan, S. Jayanti, A.R. Balakrishnan, Experimental study of air–water counter-current annular flow under post-flooding conditions, International Journal of Multiphase Flow 27-1 (2002) 51–67.

[19] S. Suzuki, T. Ueda, Behavior of liquid films and flooding in counter-current two-phase flow. Part 1: flow in circular tubes, International Journal of Multiphase Flow 3–6 (1977) 517–532.

[20] K. Takeuchi, M.Y. Young, A.F. Gagnon, Flooding in the pressurizer surge line of AP600 plant and analyses of APEX data, Nuclear Engineering and Design 192 (1999) 45–58.

[21] G.B. Wallis, One-dimensional Two-phase Flow, Mc Graw Hill, New York, 1969. pp. 336–345.

[22] G.J. Zabaras, A.E. Dukler, Counter-current gas-liquid annular flow, including the flooding state, AIChE Journal 34-3 (1988) 389–396.

[23] A. Zapke, D.G. Kroger, The influence of fluid properties and inlet geometry on flooding in vertical and inclined tubes, International Journal of Multiphase Flow 22-3 (1996) 461–472.